energies

Article

Collaborative Optimal Configuration of a Mobile Energy Storage System and a Stationary Energy Storage System to Cope with Regional Grid Blackouts in Extreme Scenarios

Weicheng Zhou *, Ping Zhao and Yifei Lu

College of Electrical Engineering & New Energy, China Three Gorges University, Yichang 443002, China; zhaoping@ctgu.edu.cn (P.Z.); 202308580121163@ctgu.edu.cn (Y.L.)
* Correspondence: 202108080021063@ctgu.edu.cn; Tel.: +86-137-6262-9963

Abstract: To address regional blackouts in distribution networks caused by extreme accidents, a collaborative optimization configuration method with both a Mobile Energy Storage System (MESS) and a Stationary Energy Storage System (SESS), which can provide emergency power support in areas of power loss, is proposed. First, a time–space model of MESS with a coupled transportation network and power grids is constructed, as a MESS is more flexible than a SESS. Considering resilience and recovery, a minimization objective function for total cost, encompassing the hybrid energy storage investment cost, the power grid operation cost, and the load shedding penalty cost, is established. Moreover, considering SESS constraints and operational constraints, a hybrid configuration model is established. Then, considering the probability of extreme accidents, the scenario analysis method is used to address randomness, ensuring that the configuration results can be adapted to various scenarios. The proposed method can fully combine the time–space flexibility of MESS and the economic advantages of SESS, which can reduce the total cost and ensure the power system's reliability. Finally, the effectiveness of the proposed method is verified by the improved IEEE33 system.

Keywords: extreme scenarios; power system optimization; mobile energy storage system; time–space constraint; energy storage optimal configuration

Citation: Zhou, W.; Zhao, P.; Lu, Y. Collaborative Optimal Configuration of a Mobile Energy Storage System and a Stationary Energy Storage System to Cope with Regional Grid Blackouts in Extreme Scenarios. *Energies* **2023**, *16*, 7903. https://doi.org/10.3390/en16237903

Academic Editor: Antonio Rosato

Received: 27 October 2023
Revised: 26 November 2023
Accepted: 1 December 2023
Published: 4 December 2023

1. Introduction

In recent years, global climate has changed dramatically, and extreme natural disasters such as rainstorms, earthquakes, and typhoons have occurred frequently, resulting in regional power outages, which has led to enormous economic loss [1,2]. The distribution network is located at the end of the power system, directly affecting the power supply's reliability in urban areas. At present, researchers are increasingly focusing on the impact of high-damage, extreme accidents on power systems, and have introduced the concept of "resilience recovery" to assess the reliability of power systems affected by extreme accidents [3,4]. As a classic regulation resource, the energy storage system has the characteristics of rapid responsiveness and strong flexibility [5]. Such systems can quickly provide emergency support in cases with power loss during disasters, thereby reducing the load shedding of users and ensuring the reliability of the power grid during extreme events. Therefore, it is important to study the configuration of energy storage systems influenced by extreme accidents to promote the construction of power systems.

Traditionally, due to the relatively mature and low-cost advantages of stationary energy storage system (SESS) technology, the distribution network usually prefers to configure SESSs to improve the resilience of the power system. In reference [6], the energy storage system configuration method based on quantitative resilience indicators was proposed to improve the seismic resistance capacity of the distribution network. Reference [7] proposed an optimization method considering the joint configuration of line reinforcement and

SESS resources to improve the resilience of the power grid under typhoon conditions. In reference [8], considering the failure rate of the distribution network, a SESS was configured to improve the resilience of the power grid. The above references show that SESSs can provide load recovery in cases of extreme accidents. However, the biggest defect is that the access location in the distribution network cannot be changed. Moreover, the occurrence of extreme faults is often accompanied by randomness, which means that blackout areas in the distribution network during extreme accidents are uncertain. Although SESS can provide certain power support under extreme conditions, it still has certain limitations as an emergency power supplier after an accident.

In recent years, with technological development, the mobile energy storage system (MESS), a new type of energy storage system, has gradually become the first choice for an emergency power supply due to its spatial mobility characteristics, flexible dispatching, easy on-site installation and operation, rapid response ability, high reliability, strong mobility, and lack of geographical restrictions compared with traditional SESS [9]. For example, during the global pandemic in 2020, MESSs, as the emergency power sources, were used to expedite power infrastructure projects, ensuring timely power for the construction of temporary hospitals and guaranteeing a reliable power supply for these medical facilities. In reference [10], a dynamic microgrid was established according to different faults, and the MESSs improved the resilience of the power grid under different fault conditions. Aiming at minimizing the cost of load shedding, reference [11] established a distribution network disaster recovery model that considered the spatial transfer, power support, and network reconfiguration constraints of MESSs; this approach reduced the load loss in the fault area through MESS scheduling. In reference [12], MESS units were configured based on a typhoon disaster model to improve the flexibility of the power grid under extreme accidents. In the above studies, MESSs were directly configured without considering the investment cost or the optimal configuration. However, currently, the construction cost of energy storage systems is high, especially the construction cost of MESSs units, which may lead to excessive investment, thereby undermining the economy of power systems. Moreover, it takes a certain amount of time for MESS-based power to reach the fault area in a power grid, which may lead to lagging power support. Therefore, reducing the economic cost of energy storage systems while ensuring the reliability of power systems is an urgent task.

In this paper, a configuration method with both MESSs and SESSs is proposed for extreme scenarios; this method combines the strengths and weaknesses of MESSs and SESSs, namely, the spatial and temporal characteristics of MESSs and the economy of SESSs. To ensure the reliability of the distribution network's power supply during extreme accidents, a resilience constraint model is established for the distribution network during the fault period. Considering the randomness of faults, the scenario analysis method is used to ensure that the configured energy storage system can satisfy the power system's requirements. Based on analyses with the improved IEEE33 node text system and comparative analysis, it is evident that the method proposed in this paper balances the reliability and economy of the configuration. The main contributions and innovations of this paper are as follows:

- A model for the joint configuration of MESS and SESS has been established, which has fully utilized the respective advantages of the two types of energy storage systems, resulting in improved economic benefits for the optimization results.
- Considering the load recovery, the reliability constraint is established in this paper, which can ensure that the energy storage configuration results can meet the load recovery requirements.
- Given the randomness of extreme scenarios, the randomness has been addressed through the method of scenario analysis, allowing the configuration results to adapt to multiple scenarios for operational efficiency.

2. Mobile Energy Storage System

2.1. Structure of MESS

An MESS is mainly composed of two parts: a power truck and a container module. The container module is generally composed of an energy storage system, a control system and a protection system, and its structure is shown in Figure 1. As the core part of the energy storage system, the battery pack releases or absorbs energy. The converter is an energy conversion device that converts the direct current of the battery into a three-phase alternating current. It can operate in both grid-connected and off-grid modes. The converter outlet is connected to the isolation transformer so that the primary side and the secondary side are completely insulated to ensure the electrical safety of the container system to the greatest extent possible. Finally, this system is connected to the power grid through a three-phase plug. The control system consists of an energy management system and a monitoring system. To ensure the safety of the overall system and to protect the energy storage containers, the container is also equipped with a firefighting system and an air conditioning system.

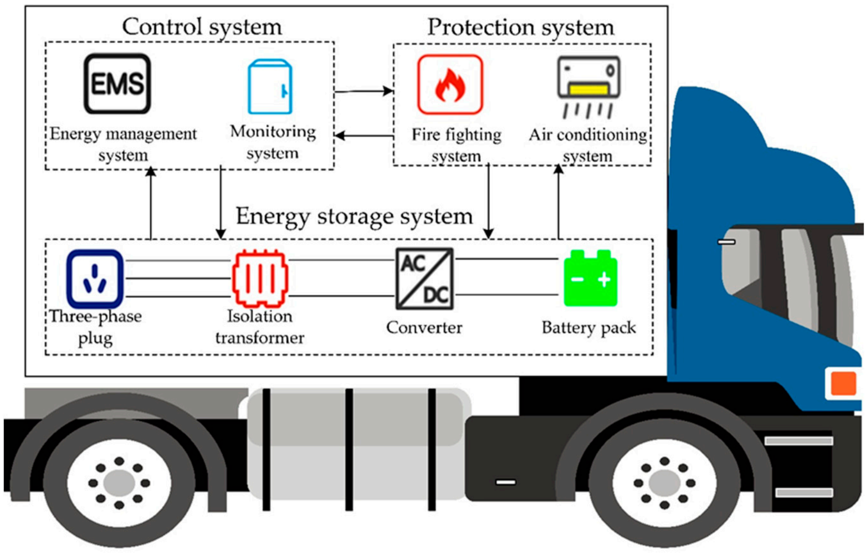

Figure 1. Structural diagram of the mobile energy storage system.

2.2. MESS Space–Time Scheduling Model

For independent distribution networks and transportation networks, researchers have established a relatively systematic theoretical basis for planning; the nodes of the transportation network and the distribution network often correspond to each other geographically, and geographical factors must be considered during the planning and layout phases for both networks. Since many nodes correspond geographically, collaborative planning often occurs [13], leading to a coupled relationship between the two networks.

In urban planning, distribution networks are commonly built along transportation networks, so there is a direct coupled relationship between these networks. In Figure 2, each distribution network node corresponds to a transportation network node. In this paper, the coordinate mapping method is used to couple and model the two networks, where each distribution network node corresponds to a traffic network coordinate. The space–time constraints of the studied MESS are shown in Equations (1)–(3):

$$D_{i,t,s} = Z \cdot n_{jk,i,t,s} \tag{1}$$

$$n_{jk,i,t,s} = \left| x_{i,t+1,s} - x_{i,t,s} \right| + \left| y_{i,t+1,s} - y_{i,t,s} \right| \tag{2}$$

$$Z \cdot n_{jk,i,t,s} \leq v_{\max} \Delta t \tag{3}$$

where the subscripts j and k represent the initial and final nodes during the MESS movement process, respectively, and Δt represents the scheduling time interval. The subscript s represents the scenario. $n_{jk,i,t,s}$ represents the number of transportation network grids in which the MESS moves from node j to node k, ($x_{i,t,s}$,$y_{i,t,s}$) are the coordinates of the corresponding distribution network node, and Z represents the unit length of the transportation network grid (the traffic distance between adjacent distribution network nodes). To simplify the processing of the road network, an equal-length square grid equivalent to that of the traffic network is used. $D_{i,t,s}$ is the distance the MESS moves at time t in scenario s, and $v_{\max}$ is the average movement speed of the MESS.

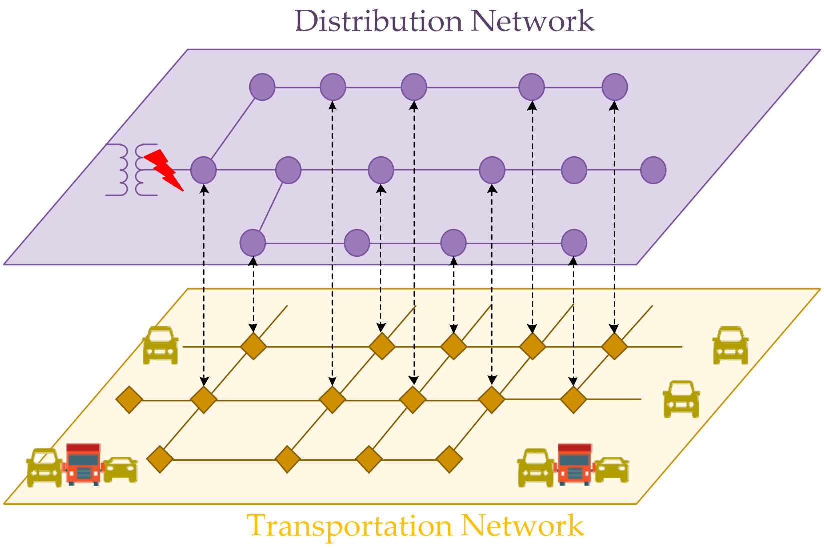

Figure 2. Diagram of the coupled distribution network-transportation network.

Equations (1) and (2) represent the space distance from the initial node j to node k, and Equation (3) indicates that the MESS cannot move more than the farthest distance possible in a unit dispatching cycle.

However, Equation (2) is a nonlinear nonconvex constraint, which will make obtaining a solution difficult [14,15]. Therefore, the model needs to be equivalently transformed into a general-form linear model. In this paper, the Big-M method is used to linearize the absolute value constraint. Assuming $w = x_{i,t+1,s} - x_{i,t,s}$, $u = y_{i,t+1,s} - y_{i,t,s}$, the linearization result is as follows:

$$\begin{cases} w + u - M(1-\delta^1_{i,t,s}) \leq n_{jk,i,t,s} \leq w + u + M(1-\delta^1_{i,t,s}) \\ w - u - M(1-\delta^2_{i,t,s}) \leq n_{jk,i,t,s} \leq w - u + M(1-\delta^2_{i,t,s}) \\ -w - u - M(1-\delta^3_{i,t,s}) \leq n_{jk,i,t,s} \leq -w - u + M(1-\delta^3_{i,t,s}) \\ -w + u - M(1-\delta^4_{i,t,s}) \leq n_{jk,i,t,s} \leq -w + u + M(1-\delta^4_{i,t,s}) \\ \delta^1_{i,t,s} + \delta^2_{i,t,s} + \delta^3_{i,t,s} + \delta^4_{i,t,s} \leq 1 \end{cases} \tag{4}$$

where $\delta^1_{i,t,s}$, $\delta^1_{i,t,s}$, $\delta^1_{i,t,s}$, and $\delta^1_{i,t,s}$ are adjustable Boolean variables (0–1 variables) reflecting the relative sizes of $x_{i,t+1,s}$, $x_{i,t,s}$, $y_{i,t+1,s}$, and $y_{i,t,s}$, respectively. For example, when both conditions $x_{i,t+1,s} \geq x_{i,t,s}$ and $y_{i,t+1,s} \geq y_{i,t,s}$ are satisfied, $\delta^1_{i,t,s} = 1$ and $\delta^2_{i,t,s} = \delta^3_{i,t,s} = \delta^4_{i,t,s} = 0$. M is a large positive number.

2.3. MESS Operational Constraint Model

A MESS can charge from or discharge to a distribution network node while satisfying the following operational constraints.

$$0 \leq P_{j,i,t,s}^{M,c} \leq \mu_{j,i,t,s}^{c} \cdot P^{M} \tag{5}$$

$$0 \leq P_{j,i,t}^{M,d} \leq \mu_{j,i,t,s}^{d} \cdot P^{M} \tag{6}$$

$$\sum_{j}^{\Omega_B} (\mu_{j,i,t,s}^{c} + \mu_{j,i,t,s}^{d}) \leq 1 \tag{7}$$

$$0 \leq E_{i,t,s}^{M} \leq E^{M} \tag{8}$$

$$E_{i,t,s}^{M} = E_{i,t-1,s}^{M} + (\eta \sum_{j}^{\Omega_B} P_{j,i,t,s}^{M,c} - \frac{1}{\eta} \sum_{j}^{\Omega_B} P_{j,i,t,s}^{M,c}) \Delta t \tag{9}$$

where P^M represents the configurable power of the MESS, E^M represents the configurable capacity of the MESS, and $\mu_{j,i,t,s}^{c}$ and $\mu_{j,i,t,s}^{d}$ represent the charging and discharging flags (0–1 variables) of the MESS at node j in scenario s, respectively. Ω_B is the set of distribution network nodes. $P_{j,i,t,s}^{M,c}$ and $P_{j,i,t,s}^{M,d}$ represent the charging and discharging powers of the MESS at node j in time span t. $E_{i,t,s}^{M}$ is the storage capacity of the i-th MESS at time t. η is the charging/discharging efficiency.

Equations (5) and (6) represent the charging and discharging constraints of the MESS at the access node, respectively, and the charging and discharging processes cannot be carried out at the same time. Equation (7) ensures that the MESS can only save electricity in one distribution network node to achieve power conversion. Equations (8) and (9) represent the energy storage capacity of the MESS at time t.

3. Configuration Model

This section mainly includes the objective function and constraints of the configuration model. Considering the investment cost, operation and maintenance cost, and load shedding penalty cost, the objective function of the collaborative configuration of the MESS and SESS is established, which can fully leverage the role of the two types of energy storage systems. The reliability constraint is used to ensure that the configuration results can meet the load recovery requirements.

3.1. Objective Function

Based on the two characteristics of economy and reliability in power systems, a three-layered objective function [16] involving the energy storage investment cost, operation cost, and load shedding penalty cost in extreme scenarios is established. This equation aims to find an economical scheme that provides a reliable power supply in multi-fault scenarios. The total cost objective function is:

$$\min F = F_{inv} + F_{op} + F_{cur} \tag{10}$$

where F represents the total cost in the system, F_{inv} represents the investment cost, F_{op} represents the operation and maintenance cost, and F_{cur} represents the load shedding penalty cost.

3.1.1. Investment Cost

The investment cost in this paper mainly refers to the construction cost of the energy storage system, which consists of two parts: capacity cost and power cost.

$$F_{inv} = F_{inv}^{M} + F_{inv}^{S} \tag{11}$$

$$F_{inv}^{M} = n_i (C_{EM} E^{M} + C_{PM} P^{M}) \tag{12}$$

$$F_{inv}^{S} = n_j (C_{ES} E^{S} + C_{PS} P^{S}) \tag{13}$$

where n_i and n_j represent the planned number of MESSs and SESSs, respectively; C_{EM} and C_{ES} represent the unit capacity cost of MESS and SESS, respectively; E^M and E^S represent the configuration capacities of the MESS and SESS, respectively; and P^M and P^S represent the configurable power MESS and SESS, respectively.

3.1.2. Operation and Maintenance Cost

The operation and maintenance cost refers mainly to the cost associated with the operation of the system, as follows:

$$F_{op} = F_{op}^{M} + F_{op}^{S} + F_{buy} \tag{14}$$

$$F_{op}^{S} = \sum_{s}^{\Omega_A} p_s [\sum_{i}^{N} \sum_{t}^{T} (\kappa^c P_{j,i,t}^{S,c} + \kappa^d P_{j,t,s}^{S,d})] \tag{15}$$

$$F_{op}^{M} = \sum_{s}^{\Omega_A} p_s [\sum_{i}^{N} \sum_{t}^{T} (\kappa^c P_{j,i,t,s}^{M,c} + \kappa^d P_{j,i,t,s}^{M,d}) + F_{fuel}] \tag{16}$$

$$F_{fuel} = \sum_{s}^{\Omega_A} p_s (\sum_{i}^{N} \sum_{t}^{T} C_{fuel} D_{i,t,s}) \tag{17}$$

$$F_{buy} = \sum_{s}^{\Omega_A} p_s (C_{buy} P_{buy}) \tag{18}$$

where p_s represents the probability of each scenario occurring, Ω_A represents the set of scenarios, κ^c and κ^d represent the charging and discharging costs of the energy storage system, respectively, and C_{buy} represents the purchasing cost of the distribution network from the main power network. P_{buy} represents the purchasing power of the distribution network via the first node of the main power network. C_{fuel} represents the unit moving cost of a MESS, and $D_{i,t,s}$ represents the moving distance of a MESS.

Equation (15) represents the SESS operational cost, which includes charging and discharging costs. Equation (16) represents the MESS operational cost. Since the MESS carrier is a large truck, certain fuel consumption costs are generated during transportation. Therefore, the operation of an MESS encompasses both charging and discharging costs along with fuel consumption expenses during transportation, as denoted in Equation (17). Equation (18) represents the power purchase cost for distribution network element nodes in the power transmission network.

3.1.3. Load Shedding Penalty Cost

The traditional optimal configuration of energy storage usually only involves two scales for planning and scheduling operations. However, in extreme scenarios, certain loads in the power system will be removed due to faults, resulting in regional blackouts in the power grid; based on previous research, the load shedding factor needs to be considered in the objective function to obtain the optimal configuration. The load shedding penalty cost is as follows:

$$F_{cur} = \sum_{s}^{\Omega_A} p_s [\sum_{t}^{T} \sum_{j}^{\Omega_B} \omega_j \kappa_L (P_{j,t}^{L} - P_{j,t,s}^{cur})] \tag{19}$$

where $P_{j,t}^{L}$ represents the predicted load value, $P_{j,t,s}^{cur}$ represents the load value removed in an extreme scenario, ω_j represents the weight of distribution network nodes, and κ_L represents the unit load shedding penalty cost.

3.2. SESS Operation Constraint Model

A SESS can charge from or discharge to a distribution network node while satisfying the following operational constraints.

$$0 \le P_{j,t,s}^{S,c} \le a_{j,t,s}^{c} \cdot P^{S} \tag{20}$$

$$0 \le P_{j,t,s}^{S,d} \le a_{j,t,s}^{d} \cdot P^{S} \tag{21}$$

$$a_{j,t,s}^{c} + a_{j,t,s}^{d} \le 1 \tag{22}$$

$$0 \le E_{j,t,s}^{S} \le E^{S} \tag{23}$$

$$E_{j,t,s}^{S} = E_{j,t-1,s}^{S} + (\eta P_{j,t,s}^{S,c} - \frac{1}{\eta} P_{j,t,s}^{S,d}) \Delta t \tag{24}$$

where P^S represents the configurable power of the SESS; E^S represents the configurable capacity of the SESS; $a_{j,t,s}^{c}$ and $a_{j,t,s}^{d}$ represent the charging and discharging flags (0–1 variables) of the SESS at node j in scenario s, respectively; Ω_B represents the set of distribution network nodes; $P_{j,t,s}^{S,c}$ and $P_{j,t,s}^{S,d}$ are the charging and discharging powers of the SESS at node j in time span t; $E_{j,t,s}^{S}$ represents the storage capacity of the SESS at time t; and η is the charging/discharging efficiency.

3.3. Reliability Constraint

In the power system planning problem, reliability should be guaranteed first while considering economy [17]. In this paper, the reliability of a power grid operation is quantified based on the load recovery rate in extreme scenarios. Reference [18] proposed a new concept of "resilience" in the power grid for extreme events such as increasingly frequent natural disasters and power outages caused by man-made attacks. This concept is used to enhance system resilience, emphasize effective resource utilization to maintain operations during inevitable failures, and enable quick and efficient system performance restoration. To ensure that the energy storage configuration results reflect a certain load recovery ability in extreme disaster scenarios, that is, the cutting load cannot be too large, in this paper, the recovery [19] index is used to measure the resilience recovery level during a disaster. R represents the system load recovery ratio that the optimal configuration must support to satisfy the reliability requirement, indicating the desired level of reliability to be achieved. The greater the value of R is, the higher the reliability requirement.

$$\frac{\int_{t_0}^{t_1} [F_0(t) - F_1(t)] dt}{\int_{t_0}^{t_1} F_0(t) dt} \times 100\% \ge R \tag{25}$$

where $F_0(t)$ represents the system load under normal conditions, and $F_1(t)$ represents the load removed under extreme conditions. t_0 and t_1 represent the fault occurrence time and end time, respectively. R represents the recovery requirement.

3.4. Other Constraints

3.4.1. Distributed Generation

In this paper, the distributed generation source is primarily wind power, and the active power output cannot exceed the predicted value.

$$0 \leq P_{j,t}^{DG} \leq P_{j,t}^{pre} \tag{26}$$

where $P_{j,t}^{DG}$ represents the active power output of wind power, and $P_{j,t}^{pre}$ represents the predicted value of wind power at time t.

3.4.2. Power Balance

For any node, the injected power is equal to the consumed power of the node load and the power flowing to the corresponding child node.

$$P_{j,t}^{DG} + P_{j,t,s}^{S,d} + P_{j,i,t,s}^{M,d} = \sum_{j \in \Omega_B, k \in \phi(j)} P_{jk,t,s} + P_{j,t,s}^{S,c} + P_{j,i,t,s}^{M,c} + (P_{j,t}^{L} - P_{j,t,s}^{cur}) \tag{27}$$

where $P_{jk,t,s}$ represents the active power of line $j-k$ at time t in scenario s, and $\phi(j)$ represents the set of nodes adjacent to node j.

3.4.3. Power Flow Constraints

For a distribution network with a radial structure, Dist-Flow power flow constraints are adopted. Dist-Flow is a nonlinear second-order cone model, and the Big-M method is used to relax the power flow constraints. The linearized power flow constraints [20,21] can be expressed as follows:

$$-z_{jk,t,s} S_{jk,\max} \leq P_{jk,t,s} \leq z_{jk,t,s} S_{jk,\max} \tag{28}$$

$$-z_{jk,t,s} S_{jk,\max} \leq Q_{jk,t,s} \leq z_{jk,t,s} S_{jk,\max} \tag{29}$$

$$-\sqrt{2} z_{jk,t,s} S_{jk,\max} \leq P_{jk,t,s} + Q_{jk,t,s} \leq \sqrt{2} z_{jk,t,s} S_{jk,\max} \tag{30}$$

$$V_{j,\min} \leq V_{j,t,s} \leq V_{j,\max} \tag{31}$$

$$\left\{ \begin{array}{l} V_{j,t,s} - V_{k,t,s} \leq M(1 - z_{jk,t,s}) + \frac{r_{jk} P_{jk,t,s} + x_{jk} Q_{jk,t,s}}{V_0} \\ V_{j,t,s} - V_{k,t,s} \geq -M(1 - z_{jk,t,s}) + \frac{r_{jk} P_{jk,t,s} + x_{jk} Q_{jk,t,s}}{V_0} \end{array} \right. , \forall (j,k) \in \Omega_B \tag{32}$$

where $P_{jk,t,s}$ and $Q_{jk,t,s}$ represent the active and reactive power transmitted by line $j-k$ at time t in scenario s; $S_{jk,\max}$ represents the maximum capacity of line $j-k$; $z_{jk,t,s}$ represents the state quantity of line $j-k$ at time t in scenario s (the normal line state is 1, and the fault line state is 0); $V_{j,t,s}$ represents the voltage of node j at time t in scenario s; V_0 is the rated voltage; and r_{jk} and x_{jk} represent the resistance and capacitance of the power line, respectively.

Equations (28)–(30) represent the linear capacity constraints after linearization, Equation (31) represents the voltage limit of each node, and Equation (32) represents the voltage constraint after linearization with the Big-M method.

4. Extreme Scenarios

This section is mainly about the randomness of extreme scenarios. The related scenarios probability is obtained using the method of scenario analysis.

The extreme scenarios considered in this paper mainly involve distribution network line faults caused by natural disasters. When configuring an energy storage system, it is necessary to consider the randomness of power system faults to obtain a reasonable energy storage configuration scheme effective in all scenarios. In [22], a model of extreme accidents in power systems was proposed, and the scenario analysis method was used to describe and address the randomness and uncertainty in power systems, including in scenario generation and remediation processes.

Any line could be disrupted under extreme conditions; therefore, to generate valid scenarios and determine the probability of failure of each line, Monte Carlo sampling technology is adopted based on line vulnerability analysis and the power system $N-1$ [23] fault principle, and nonsequential sampling schemes are considered [24]. However, generating numerous scenarios using the scenario generation method may lead to a huge computational burden and high solution complexity. To alleviate these issues, the scenario-reduction method [25] is applied to effectively establish a trade-off between computational burden and accuracy and to provide reasonable results for typical line fault scenarios. The flow chart of this approach is shown in Figure 3.

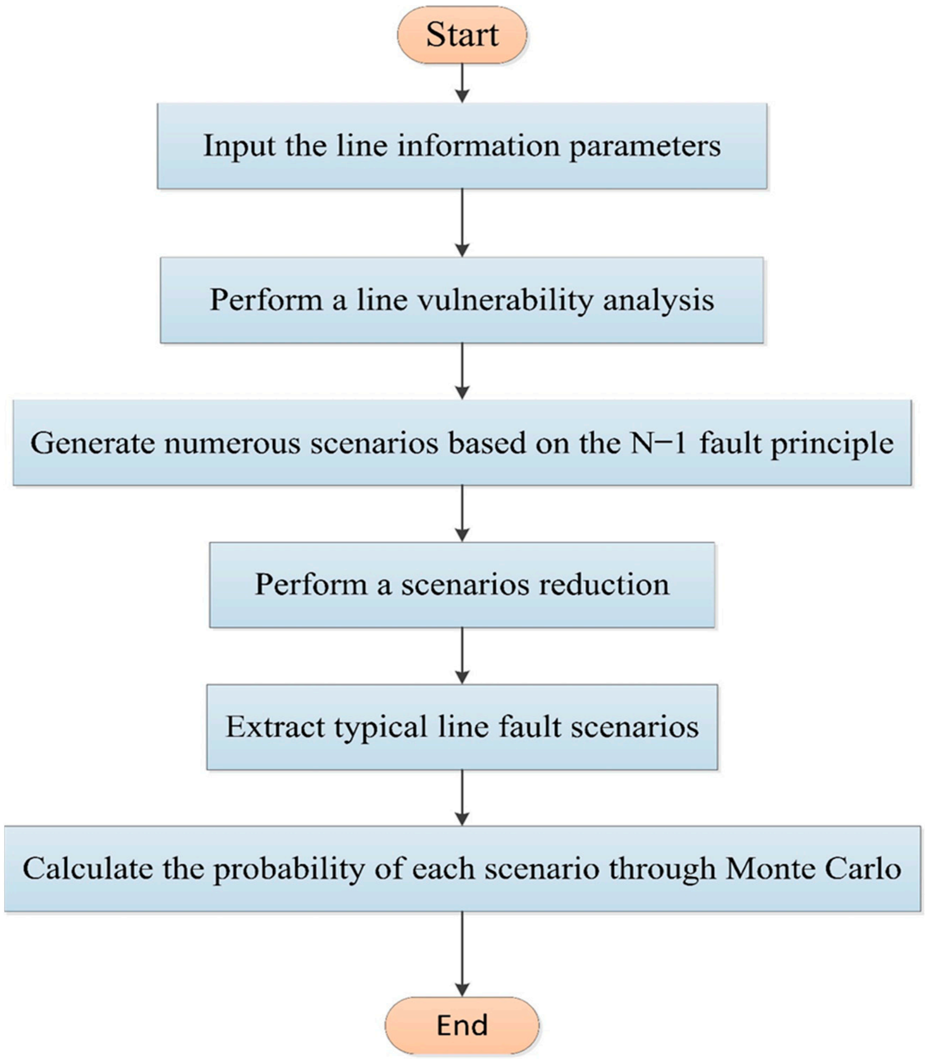

Figure 3. The extreme scenario flow chart.

5. Case Studies

5.1. Case Explanation

In order to verify the effectiveness of the proposed method, the modified IEEE33 node distribution system is selected, and the distribution network is divided into regions according to the location of the fault line, as shown in Figure 4. The three Distributed Generations (DG) in Figure 4 are wind power generation systems, and their distribution and capacity are determined through the system grid loss sensitivity and the power flow [26,27]; all three Distributed Generations have a configured capacity of 500 kW. The fault scenario set is shown in Table 1, and the determination of scenario probability is described in Section 4 of this paper. It is assumed that all extreme scenarios occur in the period of 9:00–16:00. The coupled coordinates between each node of the IEEE33 node distribution network and the transportation network are shown in Figure 5, and each distribution network node corresponds to a node in the transportation network. In this study, the loss cost of the critical load is 420 dollars/kW·h, while the loss cost of a normal load is 70 dollars/kW·h. The initial position of the MESS is optimized, and the SESS location is determined with the traditional distribution method [28,29]. Due to the proportional relationship between energy storage capacity and power, the power cost is often converted to a capacity considering only the capacity cost of energy storage. The energy storage parameters are as follows: the investment cost per unit capacity of the MESS is 280 dollars/kW·h, the investment cost per unit capacity of the SESS is 140 dollars/kW·h, the charging and discharging efficiency of the energy storage unit is 0.9, the unit charging cost of the energy storage unit is 2 dollars/kW·h, the unit discharging cost of the energy storage unit is 2 dollars/kW·h, and the fuel consumption of mobile energy storage is 5 dollars/km.

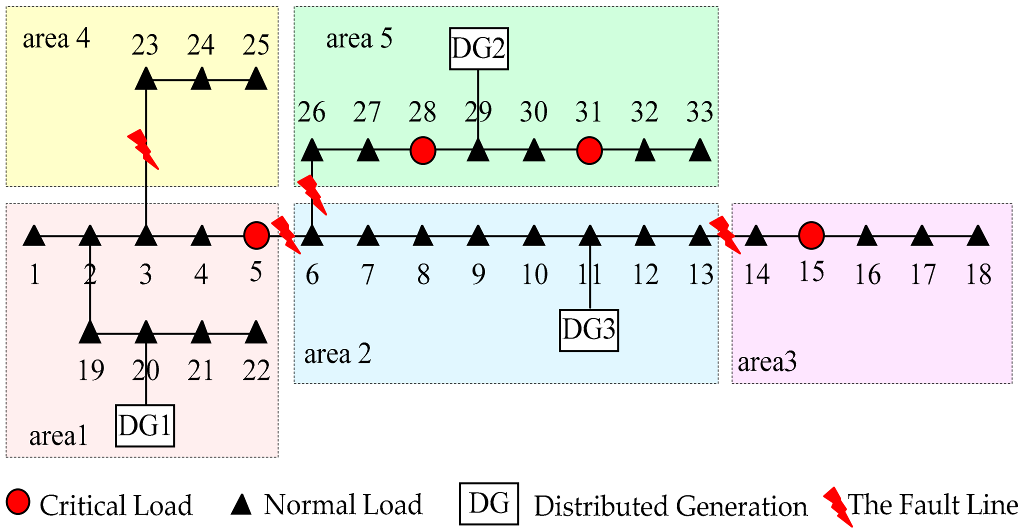

Figure 4. IEEE-33 node distribution network diagram.

Table 1. Extreme scenario set.

Scenario Number	Fault Line	Power Loss Area	Scenario Probability
1	5–6	2, 3, 5	0.213
2	13–14	3	0.204
3	3–23	4	0.305
4	6–26	5	0.278

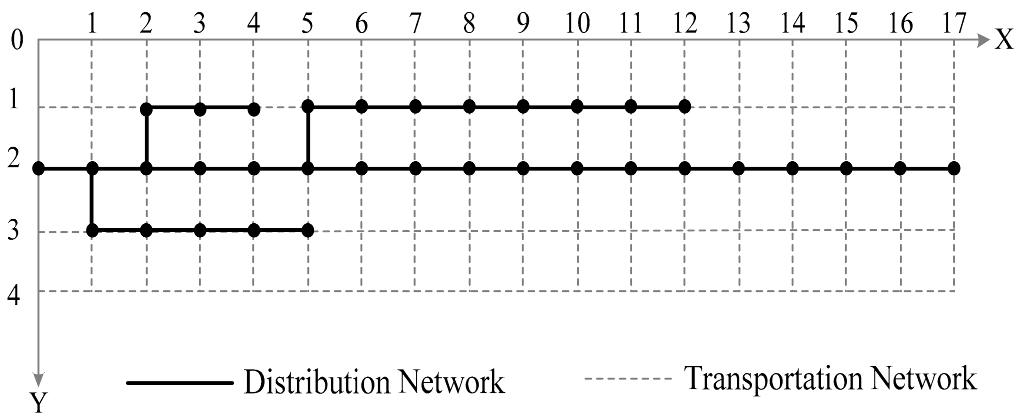

Figure 5. Diagram of coupled distribution network-transportation network coordinates.

5.2. Results and Analysis

The calculations for the case studies in this paper are based on the MATLAB R2018b platform with the YALMIP model and the CPLEX solver.

In addition to the control group, other cases with power supply load recovery ratios of more than 50%, that is, R = 50%, are considered. Reliability should be prioritized in the operation of the power system [30]. The parameters of the energy storage system are as follows: an SESS unit is based on a module with a 400 kW·h capacity that requires 100 kW of power, and an MESS unit has an 800 kW·h capacity and requires 200 kW of power. On this basis, the effectiveness of the proposed scheme is verified by designing four cases:

Case 1: Without energy storage, the power supply is recovered solely based on the distributed power sources within the distribution network (the control group).

Case 2: the SESS units are configured separately.

Case 3: the MESS units are configured separately.

Case 4: the MESS units and SESS units are collaboratively configured.

Table 2 shows the optimization results for each configuration case in extreme scenarios. Table 3 shows the energy storage configuration results for each scheme. The recovery ratio in each scenario is shown in Figure 6. The average voltage amplitude is shown in Appendix A.

Table 2. Comparison of configuration schemes in extreme scenarios.

Case	SESS Investment Cost (Dollars)	MESS Investment Cost (Dollars)	Operational Cost (Dollars)	Load Shedding Penalty Cost (Dollars)	Total Cost (Dollars)
1	\	\	15,470	1,265,068	1,280,538
2	784,000	\	16,086	434,994	1,235,094
3	\	896,000	23,905	325,192	1,246,042
4	336,000	448,000	20,412	397,152	1,201,564

Table 3. Energy storage system configuration results.

Case	SESS Results (Configured Node × Number of Configurations)	MESS Results (Configured Node × Number of Configurations)	Total Configured Capacity /kW·h
1	\	\	\
2	14×4, 16×1, 23×2, 26×5, 31×2	\	5600
3	\	5×4	3200
4	14×2, 28×3, 31×1	5×2	4000

Note: Configured node: node location of energy storage system access. Number of configurations: the number of energy storage system units configured by the node.

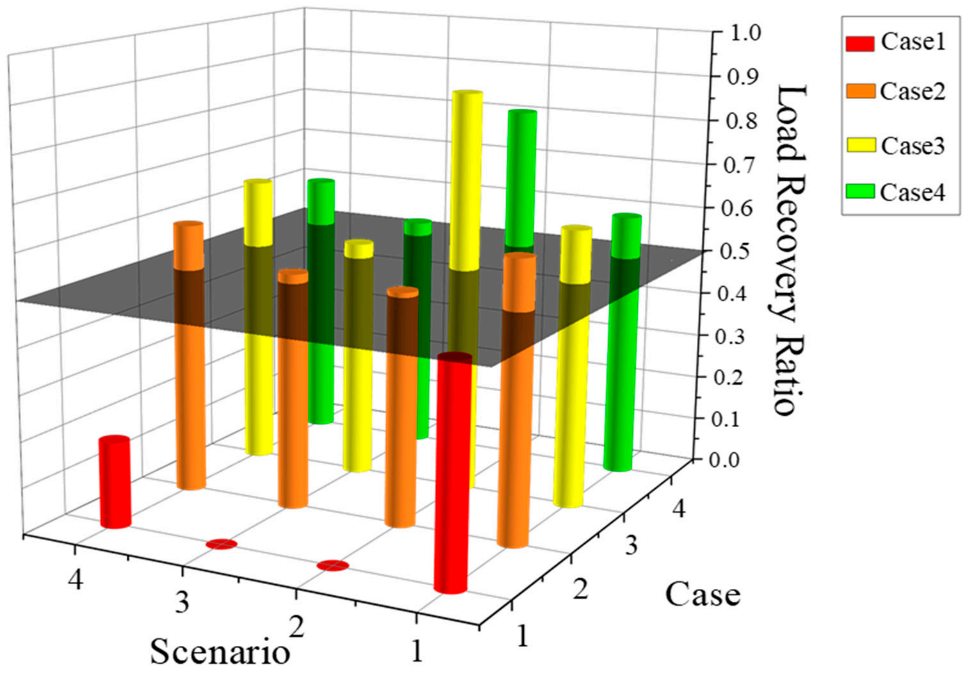

Figure 6. Load recovery ratio in different scenarios in each case.

5.2.1. Power Supply Recovery in Extreme Scenarios

As the control group, Case 1 represents the natural resilience and recovery following extreme disasters in the studied distribution network. In Case 1, no energy storage system is configured, and only the internal distributed generators are used to supply power, resulting in high load shedding loss, and the load recovery ratio in each scenario is the lowest among the values in all cases. Therefore, Case 1 does not satisfy the requirements of power supply reliability. Cases 2 to 4 demonstrate that any kind of energy storage system can provide a power supply in the distribution network. The power supply recovery in Case 3 with the MESS alone is higher than that in Case 2 with the SESS alone. This is because the MESS provides active time–space support, and space transfers can be used to effectively balance the power support among different areas and enhance the load recovery ratio of the distribution network; that is, the MESS can provide emergency power support in a fault area when a fault occurs, and the SESS can only provide power support at the access node.

The optimization results in Table 3 show that the configured position of the SESS is mainly near the critical load node, which can ensure the uninterrupted power supply for critical loads. The MESS is mobile and can meet the power supply requirements in all extreme scenarios, and its initial position is the 5th node in the distribution network, providing it with a certain distance advantage for supplying power to outage areas. With Scenario 4 as an example, the power supply recovery for different load types is shown in Table 4.

Table 4. The power supply recovery ratios.

Case	Critical Load Recovery Ratio	Normal Load Recovery Ratio
1	79.28%	40.66%
2	100%	54.17%
3	100%	59.63%
4	100%	56.48%

It can be noted that the configured energy storage system prioritizes guaranteeing the power supply reliability for critical loads and provides an uninterrupted power supply for critical loads. In practical applications, critical load nodes are associated with important facilities such as hospitals and factories.

5.2.2. Optimization Results and Economic Analysis

The results of the optimal configuration of energy storage in each scheme are shown in Table 3. Comparing Case 2 to Case 3, it is obvious that the total capacity of the separately configured SESS is much higher than that of the separately configured MESS. However, the high investment cost of the MESS leads to a higher total cost in Case 3 than in Case 2. The reliability of the independent configuration of the MESS is higher, but the total cost is not fully considered. Thus, an unbalanced relationship exists between the reliability and economy of the power system [31]. In Case 4, an approach of jointly configuring the SESS and MESS while considering the respective advantages of these two types of energy storage systems, namely, the lower investment cost of the SESS and the excellent power restoration capability of the MESS, is employed. The results show that the total cost is optimized while maintaining the reliability of the distribution network.

5.2.3. Analysis of the MESS Dispatching Results

In order to analyze the scheduling operation process of the MESS in extreme scenarios, four mobile energy storage trucks configured in Case 3 are assessed. With scenario 2 as an example for the MESS, for a line 13–14 fault, the distribution network node in the fault area loses its power supply, and the states of charge (SOC) and displacement nodes of the four mobile energy storage trucks are shown in Figure 7. For example, MESS-2 moves from the initial node to the 14th node (the fault area) and discharges from 9:00 to 11:00. Next, it moves to the 13th node to charge from 11:00 to 13:00. At 13:00, it again returns to the power loss area to supply power for 3 h (13:00–16:00). After the fault is repaired, the MESS truck returns to the initial (5th) node for charging.

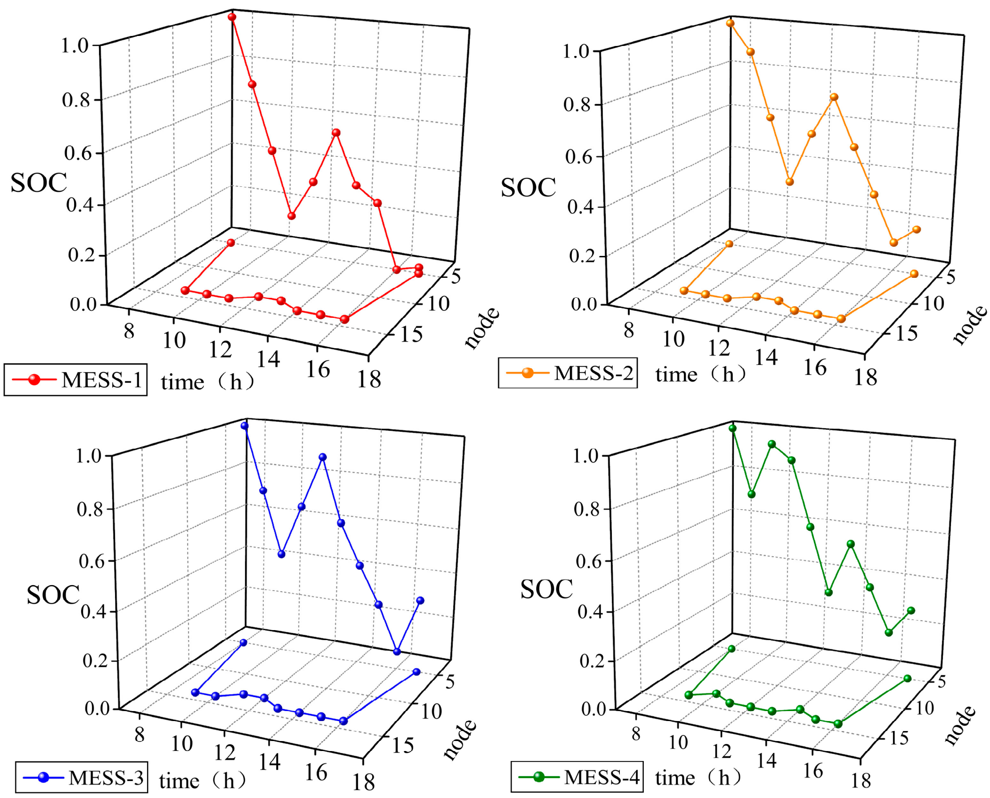

Figure 7. Diagram of the time–space dynamics of the mobile energy storage system.

5.2.4. Sensitivity Analysis

To further study the impact of the recovery ratio requirements on the total cost of the energy storage configuration, a comparison of the optimal results for different requirements is performed, as shown in Figure 8. The total cost of each scheme is proportional to the changes in the recovery ratio requirement, and the total cost in Case 4 (collaborative configuration of the MESS units and SESS units) is consistently lowest at the same recovery ratio requirement. When only one kind of energy storage system is considered, the respective advantages and disadvantages of these systems are very obvious. When the SESS units are configured separately, although the investment cost of the SESS is lower, power is only output at a fixed position, and power cannot be provided to outage areas in a timely manner. To ensure that the load recovery requirements are met in all possible scenarios, the number of SESS units that need to be configured would need to be increased accordingly, resulting in excessive investment. When the MESS units are configured separately, due to the space–time movement characteristic of the system, the MESS units can be moved to power loss areas for supply power. During an accident, MESS units can return to an area of normal operation to replenish power and then be moved to the fault area to supply power. However, the unit investment cost of the MESS is high, which leads to a higher total cost. Overall, the two types of energy storage systems are coordinated, and their respective advantages and disadvantages are effectively complementary. This approach considers the economy of SESS units and the time–space characteristics of MESS units, resulting in an optimized (minimized) total cost.

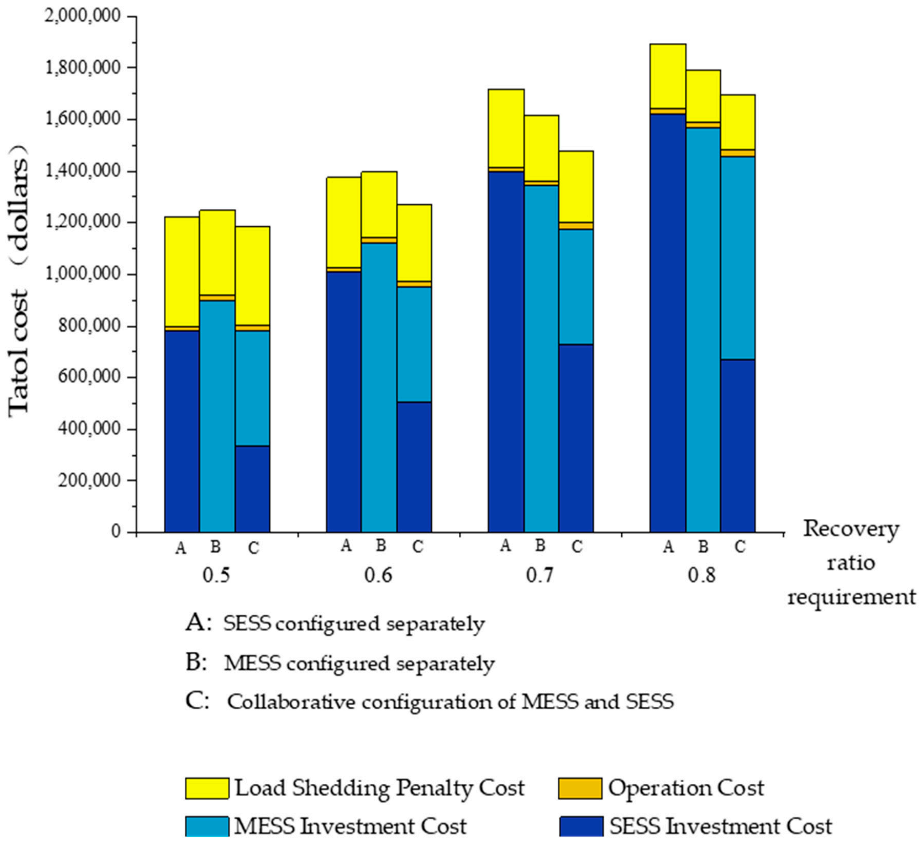

Figure 8. Optimization results for different recovery ratio requirements.

6. Conclusions

6.1. Summary

- The collaborative configuration method of two kinds of energy storage system coexistence proposed in this paper combines the time–space characteristics of MESS units and the economic advantage of SESS units. While ensuring reliability and considering economic factors, this system minimizes the total cost.

- The resilience recovery constraint proposed in this paper ensures that the optimization results of the configured energy storage system prioritize power supply reliability in the power system.
- The scenario analysis method is used to address the randomness in the generation of fault scenarios, ensuring that the results of the energy storage system configuration can be applied in various scenarios and that the power support capabilities of the energy storage system are optimal.

6.2. Future Work

With the development of power systems, the demands of power supply reliability have increased. Therefore, determining how to utilize various flexible resources to address grid faults caused by extreme disasters and to enhance the reliability of the power supply is a key focus for future research.

Author Contributions: Conceptualization, W.Z. and P.Z.; methodology, W.Z.; software, W.Z.; validation, W.Z., P.Z. and Y.L.; formal analysis, W.Z.; investigation, W.Z.; resources, W.Z.; data curation, W.Z.; writing—original draft preparation, W.Z.; writing—review and editing, W.Z.; visualization, W.Z.; supervision, W.Z.; project administration, W.Z.; funding acquisition, P.Z. All authors have read and agreed to the published version of the manuscript.

Funding: This research received no external funding.

Data Availability Statement: No new data were created or analyzed in this study. Data sharing is not applicable to this article.

Conflicts of Interest: The authors declare no conflict of interest.

Appendix A

The average voltage amplitude of Case 4 during the 24-h scheduling period is shown in Figure A1.

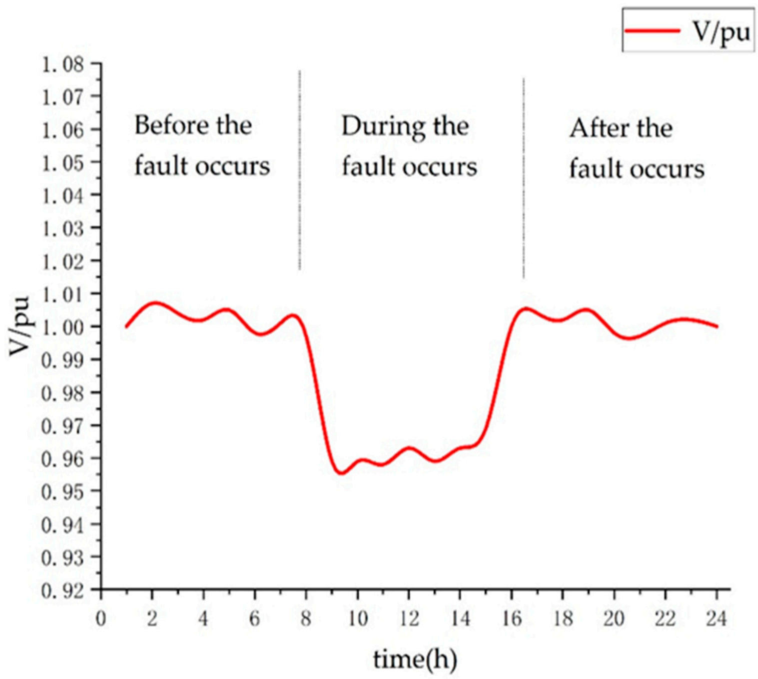

Figure A1. Voltage amplitude.

References

1. Zhang, G.; Zhong, H.; Tan, Z.; Cheng, T.; Xia, Q.; Kang, C. Texas electric power crisis of 2021 warns of a new blackout mechanism. *CSEE J. Power Energy Syst.* **2022**, *8*, 1–9.
2. Hou, H.; Yu, S.; Wang, H.; Huang, Y.; Wu, H.; Xu, Y.; Li, X.; Geng, H. Risk Assessment and Its Visualization of Power Tower under Typhoon Disaster Based on Machine Learning Algorithms. *Energies* **2019**, *12*, 205. [CrossRef]
3. Wang, Y.; Chen, C.; Wang, J.; Baldick, R. Research on Resilience of Power Systems Under Natural Disasters—A Review. *IEEE Trans. Power Syst.* **2016**, *31*, 1604–1613. [CrossRef]
4. Amani, A.M.; Jalili, M. Power Grids as Complex Networks: Resilience and Reliability Analysis. *IEEE Access* **2021**, *9*, 119010–119031. [CrossRef]
5. Wang, Y.; Xu, Y.; He, J.; Liu, C.-C.; Schneider, K.P.; Hong, M.; Ton, D.T. Coordinating Multiple Sources for Service Restoration to Enhance Resilience of Distribution Systems. *IEEE Trans. Smart Grid* **2019**, *10*, 5781–5793. [CrossRef]
6. Nazemi, M.; Moeini-Aghtaie, M.; Fotuhi-Firuzabad, M.; Dehghanian, P. Energy Storage Planning for Enhanced Resilience of Power Distribution Networks Against Earthquakes. *IEEE Trans. Sustain. Energy* **2020**, *11*, 795–806. [CrossRef]
7. Yuan, W.; Wang, J.; Qiu, F.; Chen, C.; Kang, C.; Zeng, B. Robust Optimization-Based Resilient Distribution Network Planning Against Natural Disasters. *IEEE Trans. Smart Grid* **2016**, *7*, 2817–2826. [CrossRef]
8. Ma, S.; Chen, B.; Wang, Z. Resilience Enhancement Strategy for Distribution Systems Under Extreme Weather Events. *IEEE Trans. Smart Grid* **2018**, *9*, 1442–1451. [CrossRef]
9. Yao, S.; Wang, P.; Liu, X.; Zhang, H.; Zhao, T. Rolling Optimization of Mobile Energy Storage Fleets for Resilient Service Restoration. *IEEE Trans. Smart Grid* **2020**, *11*, 1030–1043. [CrossRef]
10. Kim, J.; Dvorkin, Y. Enhancing Distribution System Resilience with Mobile Energy Storage and Microgrids. *IEEE Trans. Smart Grid* **2019**, *10*, 4996–5006. [CrossRef]
11. Yao, S.; Wang, P.; Zhao, T. Transportable Energy Storage for More Resilient Distribution Systems with Multiple Microgrids. *IEEE Trans. Smart Grid* **2019**, *10*, 3331–3341. [CrossRef]
12. Chen, Y.; Zheng, Y.; Luo, F.; Wen, J.; Xu, Z. Reliability Evaluation of Distribution Systems with Mobile Energy Storage Systems. *IET Renew. Power Gener.* **2016**, *10*, 1562–1569. [CrossRef]
13. Teng, F.; Ding, Z.; Hu, Z.; Sarikprueck, P. Technical Review on Advanced Approaches for Electric Vehicle Charging Demand Management, Part I: Applications in Electric Power Market and Renewable Energy Integration. *IEEE Trans. Ind. Appl.* **2020**, *56*, 5684–5694. [CrossRef]
14. Tang, P.; Wang, C.; Jiang, B. A Proximal-Proximal Majorization-Minimization Algorithm for Nonconvex Rank Regression Problems. *IEEE Trans. Signal Process.* **2023**, *71*, 3502–3517. [CrossRef]
15. Shen, J.; Kammara, E.K.H.; Du, L. Nonconvex, Fully Distributed Optimization Based CAV Platooning Control Under Nonlinear Vehicle Dynamics. *IEEE Trans. Intell. Transport. Syst.* **2022**, *23*, 20506–20521. [CrossRef]
16. Jiang, X.; Chen, J.; Wu, Q.; Zhang, W.; Zhang, Y.; Liu, J. Two-Step Optimal Allocation of Stationary and Mobile Energy Storage Systems in Resilient Distribution Networks. *J. Mod. Power Syst. Clean Energy* **2021**, *9*, 788–799. [CrossRef]
17. Zhao, Q.; Du, Y.; Zhang, T.; Zhang, W. Resilience Index System and Comprehensive Assessment Method for Distribution Network Considering Multi-Energy Coordination. *Int. J. Electr. Power Energy Syst.* **2021**, *133*, 107211. [CrossRef]
18. Chen, C.; Wang, J.; Qiu, F.; Zhao, D. Resilient Distribution System by Microgrids Formation After Natural Disasters. *IEEE Trans. Smart Grid* **2016**, *7*, 958–966. [CrossRef]
19. Ouyang, M.; Dueñas-Osorio, L.; Min, X. A Three-Stage Resilience Analysis Framework for Urban Infrastructure Systems. *Struct. Saf.* **2012**, *36–37*, 23–31. [CrossRef]
20. Lin, Y.; Bie, Z. Tri-Level Optimal Hardening Plan for a Resilient Distribution System Considering Reconfiguration and DG Islanding. *Appl. Energy* **2018**, *210*, 1266–1279. [CrossRef]
21. Faqiry, M.N.; Edmonds, L.; Zhang, H.; Khodaei, A.; Wu, H. Transactive-Market-Based Operation of Distributed Electrical Energy Storage with Grid Constraints. *Energies* **2017**, *10*, 1891. [CrossRef]
22. Panteli, M.; Pickering, C.; Wilkinson, S.; Dawson, R.; Mancarella, P. Power System Resilience to Extreme Weather: Fragility Modeling, Probabilistic Impact Assessment, and Adaptation Measures. *IEEE Trans. Power Syst.* **2017**, *32*, 3747–3757. [CrossRef]
23. Wang, Y.; Zhong, H.; Xia, Q.; Kirschen, D.S.; Kang, C. An Approach for Integrated Generation and Transmission Maintenance Scheduling Considering N-1 Contingencies. *IEEE Trans. Power Syst.* **2016**, *31*, 2225–2233. [CrossRef]
24. Taheri, B.; Safdarian, A.; Moeini-Aghtaie, M.; Lehtonen, M. Distribution System Resilience Enhancement via Mobile Emergency Generators. *IEEE Trans. Power Deliv.* **2021**, *36*, 2308–2319. [CrossRef]
25. Zheng, X.; Qu, K.; Lv, J.; Li, Z.; Zeng, B. Addressing the Conditional and Correlated Wind Power Forecast Errors in Unit Commitment by Distributionally Robust Optimization. *IEEE Trans. Sustain. Energy* **2021**, *12*, 944–954. [CrossRef]
26. Lu, Y.; Xiang, Y.; Huang, Y.; Yu, B.; Weng, L.; Liu, J. Deep Reinforcement Learning Based Optimal Scheduling of Active Distribution System Considering Distributed Generation, Energy Storage and Flexible Load. *Energy* **2023**, *271*, 127087. [CrossRef]
27. Li, Y.; Feng, B.; Li, G.; Qi, J.; Zhao, D.; Mu, Y. Optimal Distributed Generation Planning in Active Distribution Networks Considering Integration of Energy Storage. *Appl. Energy* **2018**, *210*, 1073–1081. [CrossRef]
28. Zhang, J.; Zhu, L.; Zhao, S.; Yan, J.; Lv, L. Optimal Configuration of Energy Storage Systems in High PV Penetrating Distribution Network. *Energies* **2023**, *16*, 2168. [CrossRef]

29. Guo, F.; Li, J.; Zhang, C.; Zhu, Y.; Yu, C.; Wang, Q.; Buja, G. Optimized Power and Capacity Configuration Strategy of a Grid-Side Energy Storage System for Peak Regulation. *Energies* **2023**, *16*, 5644. [CrossRef]
30. Wu, Y.-K.; Chen, Y.-C.; Chang, H.-L.; Hong, J.-S. The Effect of Decision Analysis on Power System Resilience and Economic Value During a Severe Weather Event. *IEEE Trans. Ind. Appl.* **2022**, *58*, 1685–1695. [CrossRef]
31. Wang, Y.; Huang, L.; Shahidehpour, M.; Lai, L.L.; Zhou, Y. Impact of Cascading and Common-Cause Outages on Resilience-Constrained Optimal Economic Operation of Power Systems. *IEEE Trans. Smart Grid* **2020**, *11*, 590–601. [CrossRef]